

# Improved numerical modelling of competitive counterion binding in polyelectrolyte solutions

William F. Moss

Department of Mathematical Sciences, Clemson University, Clemson, South Carolina 29634, USA

and H. Garth Spencer\*, George B. Savitsky and Carl M. Riedl

Department of Chemistry, Clemson University, Clemson, South Carolina 29634, USA  
(Received 22 March 1990; accepted 13 May 1990)

In a previous study of the system  $\text{Mg}^{2+}/\text{Na}^+$ /polyion, polyion = polygalacturonate, the relative suppression of the binding of  $\text{Na}^+$  by the presence of  $\text{Mg}^{2+}$  was found to be nearly linearly related to the ratio  $P_{b,\text{Mg}}/P_{b,\text{Na}}$ , where  $P_{b,\text{Mg}}$  and  $P_{b,\text{Na}}$  are the numbers of counterions per unit charge associated with or bound to the polyion, in the pure magnesium and sodium salts of the polyelectrolyte, as calculated from the relationships based on the mathematical formulation of the Poisson–Boltzmann (PB) model using the method of Peterlin and Dolar. Subsequent numerical studies involved polyions which had smaller interchange distances and the Peterlin and Dolar approach was not able to model these systems. This work describes a shooting method that successfully treats a wider range of polyion systems. The dependence of competitive counterion binding properties on representative polyelectrolyte parameters and concentration predicted by the model are also provided.

(Keywords: competitive counterion binding; polyelectrolyte; model)

## INTRODUCTION

There is strong evidence that territorial binding of counterions to polyanions in the absence of excess salts when studied by n.m.r. is consistent with the Poisson–Boltzmann (PB) model<sup>1</sup>. The PB model and a theory developed by Halle *et al.*<sup>2</sup> for the quadrupolar relaxation of counterions was shown to be consistent with <sup>23</sup>Na n.m.r. studies of sodium polygalacturonate, polymannuronate and polygaluronate in aqueous solutions by Grasdalen and Kvan<sup>3</sup>. Using essentially the same procedure, we undertook the study of competitive binding between monovalent and divalent counterions by investigating the system  $\text{Mg}^{2+}/\text{Na}^+$ /polyion, polyion = polygalacturonate<sup>4</sup>. In this system of mixed salts in a 1:1 equivalent ratio in the absence of excess salts, the preferential binding of  $\text{Mg}^{2+}$  over that of  $\text{Na}^+$  was found to be strongly concentration dependent. This preferential binding was expressed by the parameter  $\Gamma_{\text{Mg}}$ :

$$\Gamma_{\text{Mg}} = \frac{X_{\text{B}}(\text{Mg}^{2+}/\text{Na}^+)}{X_{\text{B}}(\text{Na}^+)} \quad (1)$$

where  $X_{\text{B}}(\text{Mg}^{2+}/\text{Na}^+)$  is the fraction of sodium ion territorially bound in the mixed salt  $\text{Mg}^{2+}/\text{Na}^+$ /polyanion and  $X_{\text{B}}(\text{Na}^+)$  is the fraction of sodium ion bound in pure sodium salt  $\text{Na}^+$ /polyanion at the same concentration in aqueous solution. The experimental value of  $\Gamma_{\text{Mg}}$  for the galacturonate system, which represents the relative suppression of the binding of the  $\text{Na}^+$  by the competing  $\text{Mg}^{2+}$ , decreased monotonically with the

decrease in the total concentration of the polyanion, but there was no simple relationship between  $\Gamma_{\text{Mg}}$  and concentration. At the same time  $\Gamma_{\text{Mg}}$  was found to be linearly related to the ratio  $P_{b,\text{Mg}}/P_{b,\text{Na}}$  where  $P_{b,\text{Mg}}$  and  $P_{b,\text{Na}}$  are the numbers of counterions per unit charge associated with or bound to the polyion, in the pure magnesium and sodium salts of the polyelectrolyte, respectively, as calculated from the relationships based on the mathematical formulation of the Poisson–Boltzmann (PB) model.

In subsequent work<sup>5</sup>, the  $\Gamma_{\text{Mg}}$  calculated using a numerical method based on the mathematical model of Peterlin and Dolar<sup>6</sup> also followed a practically linear relationship with  $P_{b,\text{Mg}}/P_{b,\text{Na}}$  ratio in the experimentally used concentration range of about 5–50 mM of the polyion expressed on a monomer basis. The theoretically obtained linear plot was parallel within experimental error to the experimental line of best fit, albeit the absolute magnitude of the experimental and theoretical  $\Gamma_{\text{Mg}}$  differed by about 20%. Because of this remarkable agreement between the theoretical and experimental trends in this particular system we attempted similar calculations for other systems which are under investigation in our laboratory.

However, computer errors resulted when other polyion systems such as polyacrylate and polymalonate were studied numerically. The difficulty in obtaining satisfactory results using the Peterlin and Dolar model seems to be due to the significantly lower values in the axial interchange distances,  $l$ , in these polyion systems. The polygalacturonate, polyacrylate, and polymalonate systems have  $l$  values of 0.435, 0.250 and 0.125 nm, respectively. Peterlin and Dolar divided the curve of the

\* To whom correspondence should be addressed

potential function *versus* the radial distance into 40 subdivisions. The subdivisions are exponentially spaced with the intention of having smaller intervals close to the polyion surface where the potential function is changing rapidly, while large intervals are used further away from the polyion where there is a small change in the potential function. Apparently with smaller  $l$  values, the potential function decreases much more rapidly with the increasing distance from the polyion. As a result, the exponential spacing of the subdivisions is not adequate to monitor the change in the potential function. Increasing the number of subdivisions to 50 or 60 does not give satisfactory results. The current work presents an improved method of numerical solution of the Poisson–Boltzmann equation designed to circumvent restrictions on the value of  $l$  by removing the inherent interval spacing of the Peterlin and Dolar method. The model is used to explore the concentration effects on the different polyion systems, principally focusing on the effect of the axial interchange distance,  $l$ , on  $\Gamma_{\text{Mg}}$ .

## MATHEMATICAL MODEL

For the development of the model, the polyelectrolyte solution consists of negatively charged polyions and a mixture of positively charged monovalent and divalent counterions in a solvent. The competitive accumulation of the small counterions near the polyion is of interest. Length is measured in nanometres (nm) and charge in electrostatic units. We use the mathematical formulation of Dolar and Peterlin<sup>6</sup>. The polyion is modelled as an infinitely long cylinder of radius  $a$  (nm) which carries a specified number of negative charges. Let  $1/l$  denote the number of negative charges per unit length carried by the polyion. A concentric infinite cylindrical cell of radius  $R$  (nm) surrounds a single polyion. The radius  $R$  is determined from  $c_m$ , the molar concentration of the charged group on the polyanion on a monomer basis, according to

$$R = 1/(0.6023\pi l c_m)^{1/2} \quad (2)$$

The domain of this so-called cell model, is this cylindrical cell.

It is assumed that only electrostatic forces are acting, the counterions are point charges and total charge neutrality exists inside the cylindrical cell. A cylindrical coordinate system with  $z$ -axis coincident with the axis of the polyion is used. The electrostatic potential  $\psi$  will depend only on  $r$ . In the cell model the electrostatic force is assumed to be zero at the cell boundary  $r = R$ . The potential  $\psi$  is normalized so that  $\psi(R) = 0$ . The parameters  $n_1^0$  and  $n_2^0$  denote the numbers of monovalent and divalent counterions per unit volume where the electrostatic potential is zero, and  $\bar{n}_1$  and  $\bar{n}_2$  denote the average number density of monovalent and divalent counterions per unit volume. Let  $z_1 = 1$  and  $z_2 = 2$  denote the valences of the monovalent and divalent counterions, respectively. The Poisson–Boltzmann equation for this system of charges is

$$\frac{d}{dr} \left( r \frac{d\psi}{dr} \right) = -\frac{4\pi e}{\epsilon} r \left[ z_1 n_1^0 \exp\left(\frac{-z_1 e\psi}{kT}\right) + z_1 n_2^0 \exp\left(\frac{-z_2 e\psi}{kT}\right) \right] \quad a \leq r \leq R \quad (3)$$

where  $T$  denotes the absolute temperature of the polyelectrolyte in Kelvin (K);  $\epsilon$ , the dielectric constant of the solvent;  $e$ , the charge on a proton (esu); and  $k$ , the Boltzmann constant.

At  $r = R$ , the boundary conditions are

$$\frac{d\psi}{dr}(R) = 0 \quad \psi(R) = 0 \quad (4)$$

The gradient of the potential at the surface of the polyion is related to the parameter  $l$  by

$$(d\psi/dr)(a) = 2e/\epsilon a l \quad (5)$$

The parameters  $\bar{n}_1$  and  $\bar{n}_2$  are given by

$$\begin{aligned} \bar{n}_1/n_1^0 &= 2/(R^2 - a^2) \int_a^R \exp(-z_1 e\psi/kT) r dr \\ \bar{n}_2/n_2^0 &= 2/(R^2 - a^2) \int_a^R \exp(-z_2 e\psi/kT) r dr \end{aligned} \quad (6)$$

and total charge neutrality implies that

$$1/l = (z_1 \bar{n}_1 + z_2 \bar{n}_2) \pi (R^2 - a^2) \quad (7)$$

Equation (7) can be derived from the first equation in equation (4) along with equations (3) and (5).

The equivalent fractions  $N_1^0$ ,  $N_2^0$ ,  $\bar{N}_1$ ,  $\bar{N}_2$ , the ratio  $\xi$ , dimensionless variables  $\phi$  and  $x$ , and dimensionless parameters  $\bar{R}$ , and  $\lambda$  are defined as

$$\begin{aligned} N_1^0 &:= \frac{z_1 n_1^0}{z_1 n_1^0 + z_2 n_2^0} & N_2^0 &:= 1 - N_1^0 & \bar{N}_1 &:= \frac{z_1 \bar{n}_1}{z_1 \bar{n}_1 + z_2 \bar{n}_2} \\ \bar{N}_2 &:= 1 - \bar{N}_1 & \xi &:= \frac{z_1 \bar{n}_1 + z_2 \bar{n}_2}{z_1 n_1^0 + z_2 n_2^0} & x &:= r/a \\ \bar{R} &:= R/a & \phi(x) &:= -e\psi(r)/kT & \lambda &:= e^2/\epsilon k T l \end{aligned} \quad (8)$$

Specification of  $N_1^0$  together with equations (3), (4) and (5) uniquely determines  $\psi$ ,  $n_1^0$ , and  $n_2^0$ . The average number densities  $\bar{n}_1$  and  $\bar{n}_2$  can then be found from equation (6). A more convenient dimensionless form for this problem is obtained by substituting equation (8) into equations (3)–(7).

Given  $N_1^0$ ,  $0 \leq N_1^0 \leq 1$ , find a real number  $\xi$  and a function  $\phi = \phi(x)$  which is twice continuously differentiable for  $1 \leq x \leq \bar{R}$  so that

$$\frac{d}{dx} \left( x \frac{d\phi}{dx} \right) = \frac{4\lambda x}{(\bar{R}^2 - 1)\xi} [z_1 N_1^0 \exp(z_1 \phi) + (1 - N_1^0) \exp(z_2 \phi)] \quad 1 \leq x \leq \bar{R} \quad (9)$$

$$\frac{d\phi}{dr}(\bar{R}) = 0 \quad \phi(\bar{R}) = 0 \quad (10)$$

$$\frac{d\phi}{dr}(1) = -2\lambda \quad (11)$$

Once this boundary value problem (BVP) has been solved, the fraction  $\bar{N}_1$  can be computed from

$$\bar{N}_1 = \frac{2N_1^0}{(\bar{R}^2 - 1)\xi} \int_1^{\bar{R}} \exp(z_1 x) dx \quad (12)$$

The fraction of each counterion bound to the polyion can also be computed. The thicknesses of the regions over which the monovalent and divalent counterions are bound to the polyion are denoted by  $\Delta_1$  and  $\Delta_2$  (nm) and are taken to be the diameters of the hydrated

counterions. The parameters  $Pb_1$  and  $Pb_2$  denote the corresponding fraction of each counterion bound to the polyon and are defined as

$$Pb_1 := \frac{\int_a^{a+\Delta_1} \exp\left(\frac{-z_1 e\psi}{kT}\right) r dr}{\int_a^R \exp\left(\frac{-z_1 e\psi}{kT}\right) r dr} = \frac{\int_1^{1+\Delta_1/a} \exp(z_1 \phi) x dx}{\int_1^{\bar{R}} \exp(z_1 \phi) x dx} \quad (13)$$

$$Pb_2 := \frac{\int_a^{a+\Delta_2} \exp\left(\frac{-z_2 e\psi}{kT}\right) r dr}{\int_a^R \exp\left(\frac{-z_2 e\psi}{kT}\right) r dr} = \frac{\int_1^{1+\Delta_2/a} \exp(z_2 \phi) x dx}{\int_1^{\bar{R}} \exp(z_2 \phi) x dx} \quad (14)$$

Dolar and Peterlin<sup>6</sup> do not solve this BVP. Instead, they make the further substitution  $t = \ln(x)$  and convert the BVP into a linear integral equation. Numerical solutions are obtained by approximating the integrals with a quadrature formula and by solving the resulting non-linear algebraic system using Newton's method. For small values of the parameter  $l$ , we found in our previous work<sup>5</sup> that this approach either fails to converge or produces inaccurate answers. We comment further below.

## SHOOTING METHOD

Our approach is to apply the shooting method to the BVP. The differential equation (9) and the initial conditions in equation (10) constitute an initial value problem (IVP) which depends on a parameter  $\xi$ . In the shooting method, the parameter  $\xi$  is adjusted so that the remaining boundary condition, equation (11) is satisfied.

For  $N_1^0 = 0$  and  $N_1^0 = 1$ , closed form solutions exist to the BVP,  $\xi_0, \phi_0$  and  $\xi_1, \phi_1$ , respectively. The BVP has a unique solution<sup>1</sup>. If  $0 < N_{1a}^0 < N_{1b}^0 < 1$  and  $\xi_a, \phi_a$  and  $\xi_b, \phi_b$  are the solutions to the BVP, then  $\xi_0 > \xi_b > \xi_a > \xi_1$ ,  $\phi_0(x) < \phi_a(x) < \phi_b(x) < \phi_1(x)$  for  $1 \leq x < \bar{R}$ , and  $0 < \bar{N}_{1a} < \bar{N}_{1b} < 1$ .

These statements about the BVP follow from properties of the IVP. If  $\xi_1 < \xi$ , then the IVP has exactly one solution  $\phi$  which satisfies  $\phi(x) > 0$ ,  $\phi'(x) < 0$ , and  $\phi''(x) > 0$  for  $1 \leq x < \bar{R}$ . Let  $\xi_1 < \xi_a < \xi_b$ , and let  $\phi_a$  and  $\phi_b$  be corresponding solutions to the IVP for a fixed  $N_1^0$ ,  $0 \leq N_1^0 \leq 1$ . Then

$$\phi_1(x) > \phi_a(x) > \phi_b(x) \text{ and } \frac{d\phi_1}{dx}(x) < \frac{d\phi_a}{dx}(x) < \frac{d\phi_b}{dx}(x) \text{ for } 1 \leq x < \bar{R} \quad (15)$$

Let  $0 < N_{1a}^0 < N_{1b}^0 < 1$  and let  $\xi_a, \phi_a$  and  $\xi_b, \phi_b$  be solutions to the IVP for fixed  $\xi$ ,  $\xi_1 < \xi$ , then again equation (15) holds.

Let us extend our notation momentarily and let  $\phi(x, \xi)$  denote the solution of the IVP. The shooting method and the proof of existence for the BVP depend on finding a zero of the function

$$H(\xi) := \frac{\partial \phi}{\partial x}(1, \xi) + 2\lambda \quad (16)$$

Because  $H(\xi)$  is strictly increasing for  $\xi_1 \leq \xi \leq \xi_0$  and because  $H(\xi_0) > 0$  and  $H(\xi_1) < 0$ ,  $H$  has exactly one zero for  $\xi_1 \leq \xi \leq \xi_0$ . The interval  $[\xi_1, \xi_0]$  is called a bracket

for the zero. When an accurate initial guess for  $\xi$  is available, the secant method is used for a fixed number of iterations, followed by Brent's algorithm if the secant method has not converged. Brent's algorithm provides the zero of  $H$  when a good initial guess for  $\xi$  is not available. Brent's algorithm combines the bisection method, the secant method, and inverse quadratic interpolation and must be supplied with a bracket for the zero<sup>8</sup>. This algorithm shrinks the bracket until its length is less than a specified tolerance. Once our convergence criterion has been satisfied, corresponding values for  $\bar{N}_1$ ,  $Pb_1$  and  $Pb_2$  are computed. This process defines a function  $\bar{N}_1 = G(N_1^0)$  which is strictly increasing.

The n.m.r. experiments provide  $\bar{N}_1$  values and we want to numerically approximate the corresponding values of  $N_1^0$ ,  $Pb_1$  and  $Pb_2$  by applying Brent's algorithm to the function  $F(N_1^0) := G(N_1^0) - \bar{N}_1$ . The search for a bracket is simplified by the monotonicity of  $G(N_1^0)$ . Once the zero of  $F$  has been found,  $Pb_1$  and  $Pb_2$  can be computed. Given a value for  $\bar{N}_1$ , an initial guess for  $N_1^0$  is found from an approximate inverse of  $G$  obtained by first computing a spline interpolant to  $G$ . It is advantageous to minimize the number of evaluations of  $G$  because they are expensive. Rather than use some fixed number of equispaced knots (values of  $N_1^0$ ) as is often done, we have developed a procedure for computing spline interpolants which chooses the knots adaptively according to a local error criterion. This procedure usually uses about 25 knots to produce an interpolant for  $G$  which is accurate to two places. The procedure begins by evaluating  $G$  at the endpoints  $N_1^0 = 0$  and  $N_1^0 = 1$ . Each evaluation of  $G$  requires an initial guess for  $\xi$  which is obtained by interpolating whatever  $\xi$  versus  $N_1^0$  data is currently available. We use the parametric, local monotonicity preserving, quadratic splines of Goodman and Unsworth<sup>9</sup>. All the functions we need to interpolate are monotone, and these shape preserving interpolants will be also.

For  $N_1^0 = 0$  and  $N_1^0 = 1$  there exist closed form solutions to the BVP which agree with our computed solutions to within specified accuracy. In case  $N_1^0 = 0$  or  $N_1^0 = 1$ ,  $\xi$  is computed directly from the closed form solution.  $\bar{N}_1, Pb_1, Pb_2$  and  $\phi(1)$  are computed by solving a single IVP. Let  $z = z_2$  for  $N_1^0 = 0$ , let  $z = z_1$  for  $N_1^0 = 1$ , and let  $\alpha = 1/\ln(\bar{R})$ . If  $z\lambda > 1/(1 + \alpha)$ , then<sup>10</sup>

$$\xi = 2z\lambda / (\bar{R}^2 - 1)(1 + \tau^2) \quad (17)$$

where  $\tau$  is the smallest positive solution of the transcendental equation

$$z\lambda = \frac{1 + \tau^2}{1 + \tau \cot(\tau \ln(\bar{R}))} \quad (18)$$

In case  $z\lambda \leq 1/(1 + \alpha)$

$$\xi = \frac{2z\lambda}{(\bar{R}^2 - 1)(1 - t^2)} \quad (19)$$

where  $t$  is the smallest positive solution of the transcendental equation

$$z\lambda = \frac{1 - t^2}{(1 + t \coth(t \ln(\bar{R})))} \quad (20)$$

The literature on the cell model has generally reported that  $\tau$  and  $t$  must be solutions to the transcendental equations (18) and (20), respectively. We point out that

they must be the smallest positive solutions to these equations.

To solve the IVP we set  $y_1(x) := \phi(x)$  and  $y_2(x) := x\phi'(x)$ . The IVP for the resulting first order system is solved numerically using DEPAC. DEPAC is a set of three ordinary differential equation (ODE) solvers DERKF, DEABM and DEBDF designed by Shampine and Watts<sup>7</sup>. DERKF is a fifth order variable step size Runge–Kutta code used for non-stiff and mildly stiff ODEs when derivative evaluations are not expensive. It should not be used for high accuracy, nor for answers at a great many points. DEABM is a variable order, variable step size Adams code used for non-stiff and mildly stiff ODEs when high accuracy is required. DEBDF is a variable order, variable step size backward differentiation formula code which can be used on stiff ODEs when moderate accuracy is required. DERKF and DEABM attempt to determine when their use is not suitable. Each evaluation of the function  $G$  requires the solution of the initial value problem for several different values of  $\xi$ . In the shooting method these solutions are sometimes referred to as shots. DERKF is used for all shots. The final shot is repeated with DEABM and DEBDF as a precaution in case the diagnostics in DERKF should fail. We check to see that all three sets of answers agree to desired accuracy. If DERKF produces questionable answers, the user has the option of replacing it with DEABM or DEBDF.

As discussed earlier, the Dolar and Peterlin approach is equivalent to applying the shooting method using the classical fourth order Runge–Kutta method to solve the IVPs by stepping from  $\bar{R}$  to  $\exp(t_{N-1})$ , from  $\exp(t_{N-1})$  to  $\exp(t_{N-2})$ , . . . , and finally from  $\exp(t_1)$  to 1. The important point to notice here is that the step sizes are fixed and do not change when  $l$  is changed. On the other hand the potential  $\phi$  behaves qualitatively like  $\exp[-(x-1)/l]$ . When  $l$  is small, more mesh points are needed near  $x = 1$  to track  $\phi$  accurately. Consequently, a mesh which works for moderate  $l$  is not generally suitable for small  $l$ . For small  $l$ , doubling  $N$  may not help because the number of mesh points near  $x = 1$  has not increased sufficiently. The use of DEPAC avoids the problems associated with a fixed mesh because these codes have adaptive step size control. DERKF integrates from  $x = \bar{R}$  to  $x = 1$  so that the resulting approximations to  $\phi(1)$  and  $\phi'(1)$  have specified accuracy by adaptively adjusting the step size so that its built in local error test is satisfied. The local error tolerance is set up so that desired accuracy is usually achieved at  $x = 1$ .

To achieve desired accuracy, the error tolerances must be chosen according to certain inequalities. *Abserr* and *Relerr* denote the absolute and relative error tolerances for the ODE solver, *TolH* and *TolF* denote the absolute error tolerance for the zero finders applied to  $H$  and  $F$ , respectively. Let  $\xi_a$  denote the computed zero of  $H$  for given  $N_1^0$ , and let  $N_{1a}^0$  denote the computed zero of  $F$  for given  $\bar{N}_1$ . We require that

$$\frac{|\Delta H(\xi_a)| + |H(\xi_a)|}{|H'(\xi_a)|} \leq TolH \quad (21)$$

$$\frac{|\Delta F(N_{1a}^0)| + |F(N_{1a}^0)|}{|F'(N_{1a}^0)|} \leq TolF$$

where  $\Delta H$  and  $\Delta F$  denote the error in computing  $H$  and  $F$ . All the terms in equation (21) can be estimated; in particular, we set  $|\Delta H(\xi_a)| = |\phi'(1)|Relerr + Abserr$ .

Our numerical approach has been implemented in the Apple Macintosh application PolyElectrolyte. This application is programmed in Absoft MacFortran/020 and uses double precision. The user must supply values for  $a$ ,  $c_m$ ,  $\epsilon$ ,  $T$ ,  $l$ ,  $\Delta_1$  and  $\Delta_2$ . If the user indicates that these data are new, PolyElectrolyte begins by making a table of values for  $N_1^0$ ,  $\xi$ ,  $\bar{N}_1$ ,  $Pb_1$ ,  $Pb_2$  and  $\phi(1)$ . The Commands menu allows the user to choose a value for  $\bar{N}_1$  and corresponding values for  $N_1^0$ ,  $\xi$ ,  $Pb_1$ ,  $Pb_2$ , and  $\phi(1)$  are shown on screen and written to a user named output file. The Graphs menu allows the user to obtain  $\phi$  versus  $x$  plots, and  $N_1^0$ ,  $\xi$ ,  $Pb_1$ ,  $Pb_2$  and  $\phi(1)$  versus  $\bar{N}_1$  plots. The Settings menu allows the scales of these graphs to be changed and they can be copied to a drawing or word processing application.

## RESULTS AND DISCUSSION

We applied this new approach to the three representative polyelectrolyte systems: the mixed salts of polygalacturonate ( $Mg^{2+}/Na^+/PGA$ ), polyacrylate ( $Mg^{2+}/Na^+/PAA$ ), and polymalonate ( $Mg^{2+}/Na^+/PMA$ ). The bound fractions of the counterions over a large range in  $c_m$ ,  $10^{-1}$  to  $10^{-6}$  M, and  $l = 0.425$ , 0.250 and 0.125 nm were obtained, which was not possible with the Peterlin and Dolar approach. These results demonstrate the breadth of the range of parameters that are accommodated by the model. The emphasis of the applications was on the prediction of competitive binding of magnesium and sodium in a 1:1 equivalent ratio with these polyions. The relevant parameters of these systems are given in Table 1. The  $\Delta_1$  and  $\Delta_2$  values are the literature values for the diameters of the hydrated ions of sodium and magnesium, respectively<sup>11</sup>.

Figure 1 shows the plots of  $\Gamma_{Mg}$  versus  $c_m$  in the concentration range of  $10^{-1}$  to  $10^{-6}$  M for the three systems. The plots are distinctly non-linear with the greatest curvature occurring at lower concentrations so that the extrapolation to infinite dilution is not possible. Perhaps an even more significant result is that the comparative order of  $\Gamma_{Mg}$  in the three systems differs with concentration. For example, at  $c_m = 0.1$   $\Gamma_{Mg}(PGA) > \Gamma_{Mg}(PMA) > \Gamma_{Mg}(PAA)$ ; at intermediate concentrations of  $c_m$  between 0.01 and 0.075,  $\Gamma_{Mg}(PMA) > \Gamma_{Mg}(PGA) > \Gamma_{Mg}(PAA)$ ; at concentrations lower than 0.01,  $\Gamma_{Mg}(PMA) > \Gamma_{Mg}(PAA) > \Gamma_{Mg}(PGA)$ . On the other hand, the plots of  $\Gamma_{Mg}$  versus  $P_{b,Mg}/P_{b,Na}$ , shown in Figure 2, are more nearly linear except that the PGA system gives significant deviation from linearity at concentrations less than  $10^{-5}$  M. The groupings of the  $\Gamma_{Mg}$  points increases in the order PMA > PAA > PGA indicating

**Table 1** Parameters for polyelectrolyte systems. Common:  $T = 303.15$  K,  $\epsilon_r$  (relative permittivity of water) = 76.58,  $\Delta_1 = \Delta_{Na^+} = 0.72$  nm, and  $\Delta_2 = \Delta_{Mg^{2+}} = 0.86$  nm

Systems	Parameters	
	$a$ (nm)	$l$ (nm)
$Mg^{2+}/Na^+/PGA^a$	0.5	0.435
$Mg^{2+}/Na^+/PAA^b$	0.3	0.250
$Mg^{2+}/Na^+/PMA^c$	0.3 <sup>c</sup>	0.125 <sup>d</sup>

<sup>a</sup>Reference 3

<sup>b</sup>Reference 2

<sup>c</sup>Taken as the value for PAA

<sup>d</sup>Taken as one-half the value for PAA

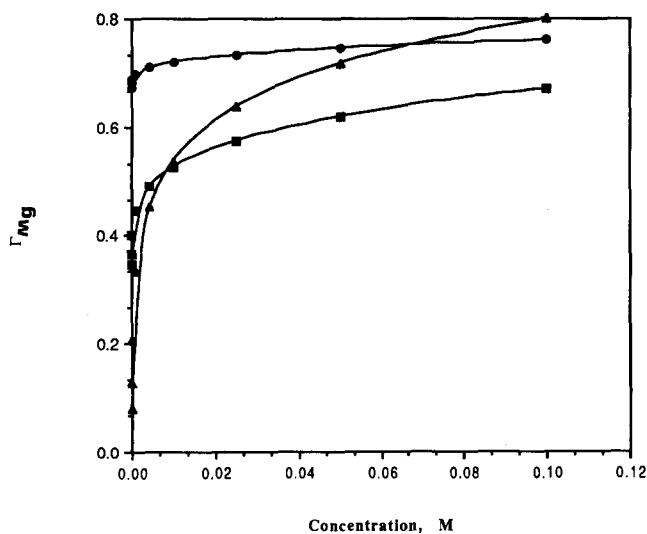


Figure 1 Concentration dependence of  $\Gamma_{Mg}$  for the mixed neutral salt systems containing equivalent amounts of  $Na^+$  and  $Mg^{2+}$ : ( $\blacktriangle$ ), PGA; ( $\blacksquare$ ), PAA; and ( $\bullet$ ), PMA

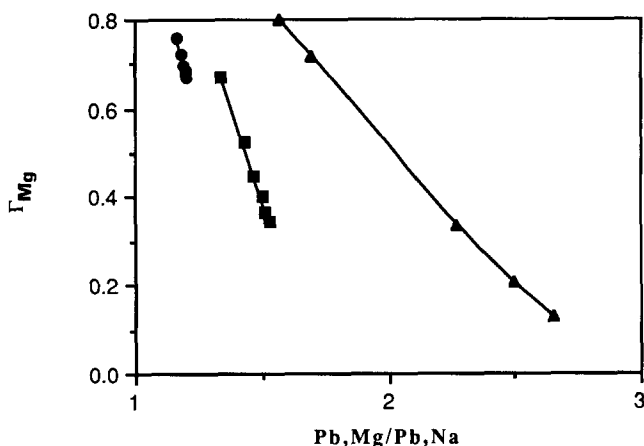


Figure 2 Plots of  $\Gamma_{Mg}$  versus  $P_{b,Mg}/P_{b,Na}$  for the mixed neutral salt systems containing equivalent amounts of  $Na^+$  and  $Mg^{2+}$  for a concentration range of  $10^{-6}$  to  $10^{-1}$  M: ( $\blacktriangle$ ), PGA; ( $\blacksquare$ ), PAA; and ( $\bullet$ ), PMA

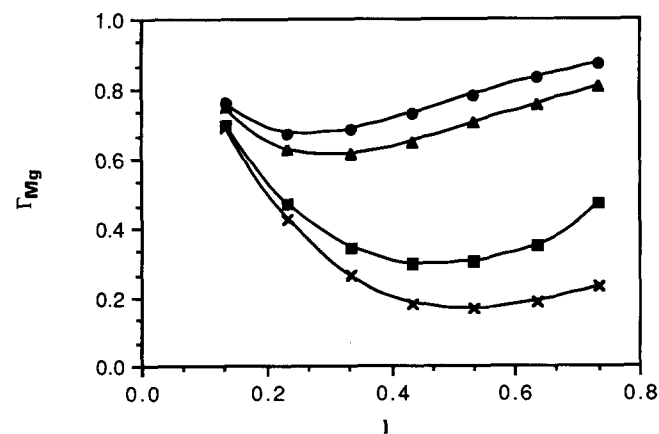


Figure 3 Plots of  $\Gamma_{Mg}$  versus  $l$  for hypothetical mixed neutral salt systems containing equivalent amounts of  $Na^+$  and  $Mg^{2+}$  at different concentrations,  $c_m$ , with parameters  $a = 0.3$  nm,  $l = 0.435$  nm,  $T = 303.15$  K,  $\Delta_1 = 0.72$  nm and  $\Delta_2 = 0.86$  nm: ( $\bullet$ ), 0.1 M; ( $\blacktriangle$ ), 0.05 M; ( $\blacksquare$ ), 0.001 M; and ( $\times$ ), 0.0001 M

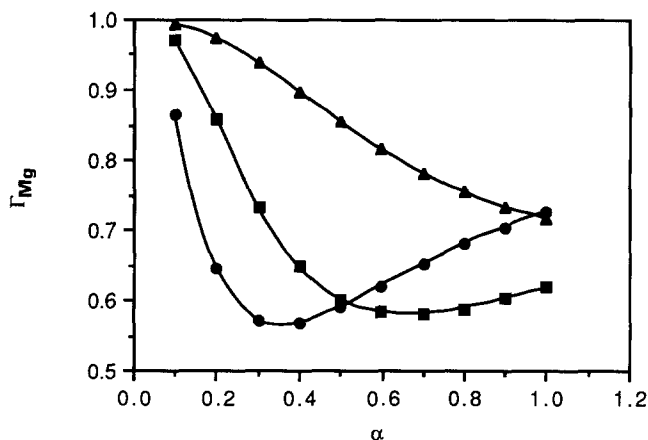


Figure 4 Plots of  $\Gamma_{Mg}$  versus degree of neutralization,  $\alpha$ , by a mixed base containing equivalent amounts of  $Na^+$  and  $Mg^{2+}$ : ( $\blacktriangle$ ), PGA; ( $\blacksquare$ ), PAA; and ( $\bullet$ ) PMA

that the competition between  $Mg^{2+}$  and  $Na^+$  is the least concentration dependent for the PMA system and the most concentration dependent for the PGA system.

Because the  $l$  parameter is the factor that most dramatically distinguishes the three systems, the effects of  $l$  and  $c_m$  on  $\Gamma_{Mg}$  for a hypothetical system in which all other parameters were held constant ( $a = 0.3$  nm,  $\Delta_1 = 0.72$ ,  $\Delta_2 = 0.86$ ) were investigated. Figure 3 is a plot of  $\Gamma_{Mg}$  versus  $l$ . The following features are of note. First of all, the concentration dependence of  $\Gamma_{Mg}$  is the smallest for low values of  $l$  and becomes more significant with increasing  $l$ . Also, the absolute value of  $\Gamma_{Mg}$  for any given concentration passes through a different minimum for the given concentration.

Figure 4 is a representation of  $\Gamma_{Mg}$  versus  $\alpha$  for the three systems of interest where  $\alpha$  is the degree of neutralization of the polyacids by a mixed base containing a 1:1 equivalent ratio of magnesium and sodium. As a polyacid is neutralized, the average distance between the charges developed during neutralization,  $l$ , decreases as  $c_m$  increases. A rigid rod conformation is assumed throughout the neutralization. As seen in Figure 4, the result of the change in these two parameters on the degree of competition depends on the system of interest and the degree of neutralization. The PAA and PMA systems exhibit  $\Gamma_{Mg}$  minima at different degrees of neutralization while PGA exhibits only an inflection. If the binding is exclusively territorial and the (PB) model is applicable, the model predicts that the competitive effect of  $Mg^{2+}$  on the binding of  $Na^+$  is minimal for small  $\alpha$ , or low pH, and significantly greater for higher  $\alpha$ , or higher pH. For the PMA and PAA this effect would be most prominent at intermediate values of  $\alpha$  where minima occur.

In summary, the model developed here predicts complicated behaviour for the competitive binding of mixed divalent and monovalent counterions with these representative polyions. The approach provides a means of calculating competitive binding properties over a broad range of parameters. Experimental results can be compared with the model and results deviating from behaviour predicted by the model can then be ascribed to effects not contained in it, such as the dependence of conformation on the degree of ionization and site binding.

REFERENCES

- 1 Fuoss, R. M., Katchalsky, A. and Lifson, S. *Proc. Natl. Acad. Sci. USA* 1951, **37**, 579
- 2 Halle, B., Wennerstrom, H. and Piculell, L. *J. Phys. Chem.* 1984, **88**, 2482
- 3 Grasdalen, H. and Kvan, B. J. *Macromolecules* 1986, **19**, 1913
- 4 Qian, C., Asdjodi, M. R., Spencer, H. G. and Savitsky, G. B. *Macromolecules* 1989, **22**, 995
- 5 Riedl, C., Qian, C., Savitsky, G. B., Spencer, H. G. and Moss, W. F. *Macromolecules* 1989, **22**, 3983
- 6 Dolar, D. and Peterlin, A. *J. Chem. Phys.* 1969, **50**, 3011
- 7 Shampine, L. F. and Watts, H. A. DEPAC – design of a user oriented package of ODE solvers, SAND-79-2374, Sandia Laboratories, 1979
- 8 Forsythe, G., Malcolm, M. and Moler, C. B. 'Computer Methods for Mathematical Computations', Prentice-Hall, Englewood Cliffs, NJ, 1967
- 9 Goodman, T. N. T. and Unsworth, K. 'Shape Preserving Interpolation by Parametrically Defined Curves', Computer Science Report, University of Dundee, 1986
- 10 Einevoll, G. and Hemmer, P. C. *J. Chem. Phys.* 1988, **89**, 474
- 11 Israelachvili, J. N. 'Intermolecular and Surface Forces', Academic, London, 1985